



Research on Source-Load Cooperative Optimization Configuration for Combined Solar and Air Source Heat Pump System Based on Demand Response

Jialin Yu, Ruyue Han^(✉), Dongmin Xi, and Yuanyuan Xu

College of Electric Power, Inner Mongolia University of Technology, Hohhot 010080, China
hanry1979@163.com

Abstract. With the promotion of the national coal to electricity policy, the installation scale of heat storage and electric heating equipment is getting bigger and bigger. The “Solar energy +” operation mode is an effective way to solve the problem of new energy consumption and reduce the cost of heating and electricity charges. To solve the problems in the planning and operation of a solar-heat pump joint operation system based on demand-side response, a two-layer optimized configuration model is proposed. First, the working characteristics of solar-air source heat pump are analyzed to fully tap the potential of electricity and heat demand response. Secondly, with the lowest annual investment and operation cost of centralized electric heating system and the lowest cost of thermal user respectively as the optimization objectives, the two-layer optimization model of regenerative electric heating based on time-sharing electricity price and user satisfaction is established, and the PSO + toolbox is used to solve the model. Finally, based on the actual data of Wulanchabu city, the results show that the double-layer optimization based on the demand side response can not only have economic benefits, but also improve the energy efficiency ratio of solar-air source heat pump, reduce the cost and better absorb the new energy.

Keywords: Solar + · DR · Bi-level Optimal · PSO

1 Introduction

With the promotion of clean, low-carbon and internationalization of energy application, the international community attaches great importance to the clean heating strategy [1]. Using solar energy, wind energy, air energy and other renewable energy to replace the traditional energy will become the mainstream direction of future heating development. The western Inner Mongolia has high altitude, low cloud capacity, long sunshine time,

Fund Project: Natural Key Research Project of Inner Mongolia University of Technology (ZZ202018); Natural Key Research Project of Inner Mongolia University of Technology (RZ2100000528); Inner Mongolia Autonomous Region Science and Technology Plan Project (N08814).

© State Grid Electric Power 2023

P. Zeng et al. (Eds.): CUS-EPSA 2022, LNEE 1030, pp. 402–416, 2023.

https://doi.org/10.1007/978-981-99-1439-5_36

abundant solar and wind energy resources, and has the natural conditions for clean heating. During the 14th Five-Year Plan period, Baotou city, relying on the construction plan of National Development and Reform Commission, built a total of 600,000 kW; 248.1 mu of ground built a solar thermal mirror field with an area of 71,000 square meters and a heating area of 355,000 square meters.

Solar energy and wind energy have certain intermittent and randomness, so it is difficult for a single energy heating to solve many problems encountered in the demand side. If the form of multi-energy complementary is adopted, so that various energy sources can learn from each other, it can make up for the shortage of a single energy heating mode [2]. Recently, the research of multi-energy complementary heating system has achieved remarkable results. Liu Qingyu et al. [3] designed the solar auxiliary heating system, combined with the solar-biomass energy combined auxiliary heating system to heat the building. Zhang Furen et al. [4] established a rural biogas and solar combined heating system, which was compared with the traditional rural coal-fired heating system, indicating that the rural biogas and solar combined heating system has strong heating capacity and stable operation. Freeman et al. [5] used TRNSYS software to simulate three non-direct-series, parallel and hybrid solar heat pump systems. The research shows that the solar-air source heat pump parallel operation system has the best heating effect and the highest energy efficiency, so it is widely used. Many scholars have conducted in-depth research on the operation characteristics and control strategy of solar-heat pump dual heat source system. By studying the heating characteristics of the constructed solar energy-air source heat pump system, the best mixed heating effect of the heat storage tank and the air source heat pump is verified [6]. Zhang Xiaoyue et al. [7] put forward a time-based control strategy for the solar air source heating system, and found that the highest energy efficiency ratio of the system can reach 7.22, the highest solar energy contribution rate is 63.69%, and the heating coefficient of the heat pump unit is 2.91. Zhu Caixia [8] established the capacity matching and operation synchronous optimization model of the solar energy and air source heat pump parallel heating system, optimized the collector area, the capacity of the heat pump and the start-stop temperature of the heat pump at the same time, and gave the optimized matching capacity and operation control strategy.

To sum up, a large number of scholars use fixed values in the optimization process of the heat load of the solar-air source heat pump joint operation system, and do not consider the tunability of user needs. In addition, with the sharp increase of electric heating users, the load characteristics of users are changed, the peak and valley difference is increased, and the utilization rate of equipment is reduced. The application of demand response technology can effectively realize peak shifting and valley filling, and improve the operation efficiency of the solar-heat pump joint operation system.

Owing to the electric heating side and heat load side using energy is different, and the response mechanism is also different. There is an interactive relationship between the two parameters, so this paper adopts bi-level optimization method, the upper time-sharing price with system annualized cost minimum goal, using particle swarm algorithm for the solar collector area, heat pump rated capacity, heat pump, heat storage tank operating power optimization, the lower consider user satisfaction of heating cost minimum as the

goal, optimize the heat load curve and feedback back to the upper, iterative system optimal capacity configuration and operation scheme. Compared with the previous research on solar-heat pump system, this paper has the following innovations:

- (1) Establishing a two-tier interaction model between users and thermal storage electric heating to reduce the cost of heating systems with better economic benefits while satisfying user satisfaction.
- (2) Considering the dual demand-side response, the response of the electric heating system to the grid-side time-of-use tariff, and the response of the heat users to the comfort and economy, effectively improves the heating quality.

2 System Structure and Mathematical Model

The structure of the solar-air source heat pump combined operation system with a heat storage device (see Fig. 1). Among them, the role of the heat storage device is to flexibly adjust the output power of the heating device, so that the electric heating heat output at different moments to achieve the ideal value, to improve the system COP (Coefficient of Performance).

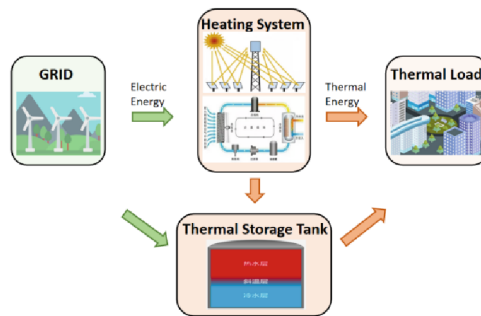


Fig. 1. Parallel system structure

In regular weather, solar energy is sufficient during the day, the heat is supplied by solar collectors and the heat is stored in the heat storage tank; at night, the heat is supplied by the heat pump and the heat is discharged from the heat storage tank. In case of extreme weather when solar energy cannot supply heat, the heat storage tank and heat pump are combined to supply heat, with the storage tank giving priority to heat release and using nighttime valley electricity for heat storage.

2.1 Solar Collector

Solar collector selection is the key to solar and air source heat pump systems, this paper selected flat plate collectors for modeling, its higher heat transfer efficiency, and less system components, simple and compact structure, with high collector efficiency, the system evaporation temperature can be maintained in a higher temperature range, the

system performance will also be improved, and in practice the flat plate collectors are more suitable for cold areas [9].

Flat-plate solar collectors are mainly composed of heat-absorbing plates, transparent covers, heat insulation layers and shells, etc. [10]. When the flat-plate solar collector works, solar radiation through the transparent cover, projected on the heat-absorbing plate, absorbed by the heat-absorbing plate and converted into heat energy, and then transferred to the heat-transferring mass inside the heat-absorbing plate, so that the temperature of the heat-transferring mass rises, as the useful energy output of the collector; at the same time, the temperature rises after the heat-absorbing plate through conduction, convection and radiation and other ways to the surrounding heat loss, which becomes the collector. Collector heat collection can be expressed as follows.

$$Q_{solar} = I\eta A/1000 \quad (1)$$

$$\eta = 0.77 - 4.47(T_{solar} - T_{out})/I \quad (2)$$

In the formula:

Q_{solar} -solar collectors heat collection, J;

I -solar radiation intensity, W/m²;

A -heat collection area, m²;

H -solar collectors collecting efficiency;

T_{solar} 、 T_{out} -water temperature and ambient temperature, °C.

2.2 Air Source Heat Pump

ASHP (Air Source Heat Pump) systems use the inverse Carnot principle to transfer the energy from the air to the water, instead of heating it directly with electric heating elements, so its energy efficiency can reach more than 4 times that of electric water heaters. ASHP uses electric energy as the circulating power to effectively absorb the unavailable low-level heat energy in the air through the heat transfer medium, and convert the absorbed heat energy into usable high-level heat energy to be released into the water. The compressor converts the low-temperature, low-pressure gaseous refrigerant into a high-pressure, high-temperature gaseous state, the compressor compression function converts heat to Q_1 , the high-temperature, high-pressure gaseous refrigerant and water for heat exchange, and the high-pressure refrigerant is cooled and condensed to a liquid state at room temperature. This process, the refrigerant heat released to heat the water, so that the water warms up into hot water. The heat absorbed by the water is Q_3 , high pressure liquid refrigerant through the expansion valve decompression, pressure drop, back to a lower temperature than the outside world, with the ability to absorb heat evaporation. Low-temperature low-pressure liquid refrigerant through the evaporator (air heat exchanger) to absorb the heat of the air itself evaporated from the liquid state into a gaseous state, the refrigerant absorbed heat from the air for Q_2 . Absorbed heat of the refrigerant into low-temperature low-pressure gas, and then inhaled by the compressor for compression, and so on and so forth cycle, and constantly absorb heat from the air, and in the heat exchanger, hot water. (see Fig. 2).

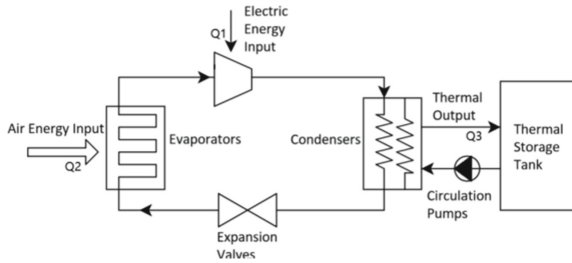


Fig. 2. Schematic diagram of ASHP

$$H_{HP}(t) = c \cdot P_{HP}(t) \quad (3)$$

In the formula:

$H_{HP}(t)$ -heat pump heat power at time t , kW;

c -COP;

$P_{HP}(t)$ -electric power consumption of heat pump at time t , kW.

2.3 Heat Storage Tank

The storage tank is a common heat storage device in wind power heating. When the heat producing equipment has heat left after meeting the heating demand, the storage tank can be regarded as a “user” to store the excess heat; when the heat producing equipment cannot meet the heating demand, the storage tank can be used as a heat source to release the stored heat to heat the user. Depending on the form of storage, there are three main basic methods of storing thermal energy: sensible heat storage, latent heat storage and thermal chemical energy storage [11]. Among them, sensible heat storage is the simplest and most common thermal energy storage system, mainly used to store thermal energy below 150°C, which is usually only used for heating because of the low efficiency of conversion into other forms of energy. This kind of heat storage is small in scale and has little impact on the environment. Considering the technical maturity, economy and other factors, the sensible heat storage with water as the heat storage medium is currently the most widely used in heat storage devices at home and abroad [12].

Commonly used water as a storage medium for heat storage tank structure (see Fig. 3), according to the needs of the heating system to determine its volume, height and maximum heat storage and release capacity and other parameters. The heat storage capacity of the heat storage tank is related to the volume, inlet and return water temperature and other parameters, and is usually calculated using the formula $Q = mcr\Delta t = \rho Vcr\Delta t$.

Generally, the larger the heat storage capacity, the higher the unit’s peaking capacity, but the corresponding investment will also increase, so it is necessary to plan its optimal capacity to improve the economy.

The heat storage tank is used to store heat during the time when the electricity price is low and release heat during the time when the electricity price is high and when

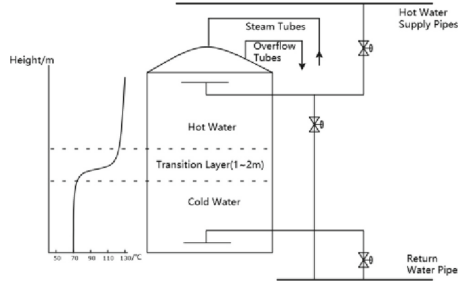


Fig. 3. Schematic diagram of the heat storage tank

the power supply is interrupted, and retain the original buffering effect. To reflect the applicability of the method proposed in this paper, the change in water temperature of the storage tank is converted to heat change in this paper. Heat storage tank characteristics can be expressed as the relationship between heat storage, heat storage/exhaust power and heat loss.

$$W_{HWT}(t + 1) = [H_{HP}(t) + H_{SP}(t)] \cdot \Delta t - W_{loss}(t) + W_{HWT}(t) \tag{4}$$

In the formula:

$W_{HWT}(t)$ -the amount of heat stored in the heat storage tank at moment t, kWh;

Δt -a time interval, 1 h;

$H_{HP}(t)$, $H_{SP}(t)$ -thermal power of ASHP and solar collector, kW;

$W_{loss}(t)$ -thermal loss at time t, kWh.

2.4 Heat Consumer

$$\frac{dT_{in}}{dt} = \frac{T_{out} - T_{in}}{R_a C_a} - \frac{Q_{aw}}{C_a} \tag{5}$$

In the formula:

Q_{aw} -system heat production, J;

T_{in} , T_{out} -inside and outside temperature, °C;

R_a -building equivalent thermal resistance, °C/kW;

C_a -building equivalent thermal capacity, kJ/°C.

3 Optimization Model

Under the condition of not considering the electricity price factor, the operation strategy of heat pump hot water unit mostly adopts temperature difference control, and for parallel heating system, the heat pump unit mostly runs in the night with low temperature and high humidity, and the operation environment is poor. In this paper, we adopt the dual control strategy of temperature and electricity price, the heat pump starts and stores heat under the condition that the water temperature is not lower than the limit value but the electricity price is low, which can reduce the influence brought by the heat pump

frost, and the heat is released by the heat storage tank under the ultra-low temperature condition, so that the heat pump always runs at a higher COP. In this paper, the all-day hourly operating power of the three units of solar collector, heat pump and heat storage tank is taken as the optimization variable, and the most value of the operating power is taken and a margin of 10% is guaranteed as the optimized capacity. The following figure shows the bi-level planning model (see Fig. 4).

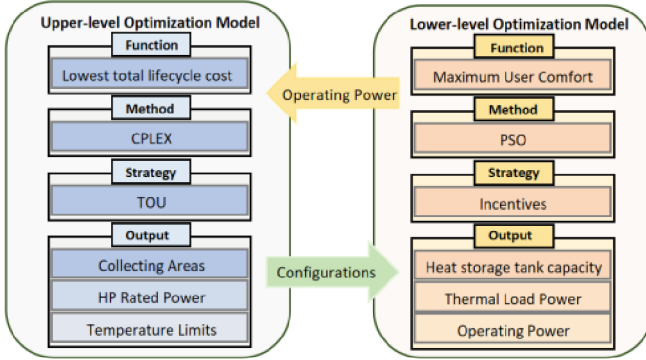


Fig. 4. Bi-level optimized configuration model

3.1 Upper-Level Problem

The upper-level planning model uses the solar collector area, the rated capacity of the heat pump, and the storage tank volume as optimization variables, and the lowest annualized cost of building the system as the objective function.

$$MinJ_1 = Min(C_c r / [1 - 1/(1+r)^l] + \sum_{i=1}^N (C_{OM,i} + C_{s,i})) \tag{6}$$

In the formula:

- C_C -system initial investment cost, ¥;
- $C_{OM,i}, C_{s,i}$ -day i construction and operating costs, ¥;
- r -discounted rate;
- N -Heating days in the year.

$$C_C = (A_{so}C_{so} + R_{HP}C_{HP} + V_{st}C_{st} + C_{else}) \tag{7}$$

In the formula:

- A_{SO} -design area of the collector, m^2 ;
- C_{SO} -collector unit area cost, $¥/m^2$;
- R_{HP} -total heating power of ASHP, kW;
- C_{HP} -unit power equipment cost, $¥/kW$;
- V_{st} -Heat storage tank volume, m^3 ;

C_{st} -equipment cost per unit volume, ¥/m³;

C_{else} -other accessories costs, ¥/kW°.

$$C_{OM} = \sum_{t=1}^T (F_{solar,t} + F_{air,t} + F_{st,t}) + F_{else} \quad (8)$$

$F_{solar,t}$, $F_{air,t}$, $F_{st,t}$, F_{else} -the solar collector, ASHP, thermal storage tank operating cost and fixed costs, ¥.

The operation cost of heat collection system is determined by its operation time and the power of heat collection circulation pump; the operation cost of heat pump unit is determined by its operation time and the power of unit and heat pump circulation pump; the operation cost of heat storage tank is determined by its opening time and heat storage power. The calculation model of each component is as follows.

$$F_{solar,t} = C_{TOU,t} \cdot P_{solar,t} \cdot t \quad (9)$$

$$F_{air,t} = C_{TOU,t} \cdot P_{air,t} \cdot t \cdot \delta_t \quad (10)$$

$$F_{st,t} = C_{TOU,t} \cdot P_{st,t} \cdot t \quad (11)$$

$C_{TOU,t}$ -the TOU electricity price at time t, ¥;

$P_{HP,t}$, $P_{SP,t}$, $P_{st,t}$ -the solar collector, ASHP, thermal storage tank running power, kW;

δ_t -heat pump start and stop coefficient.

3.2 Upper-Level Constraints

$$Q_{solar} + Q_{air} = Q_{st} + Q_{load} + Q_{loss} \quad (12)$$

$$0 \leq P_{air,t} \leq P_{air,max} \quad (13)$$

$$H_{HP}(t) \leq Q_{HP}(t) \quad (14)$$

$$\delta_t = \begin{cases} 0 & T_{tank} > T_{max} \\ 1 & T_{tank} < T_{min} \end{cases} \quad (15)$$

$$S_{min} \leq S_t \leq S_{max} \quad (16)$$

$$S_t = S_{t-1} + Q_{aw,t} - H_{load,t} \quad (17)$$

3.3 Lower-Level Problem

The lower level aims at the lowest customer heating costs within the constraint of meeting customer comfort.

$$\min J_2 = \sum_{t=1}^{24} C \cdot H_{h,t} \quad (18)$$

The relationship between heat load demand and indoor temperature is as follows:

$$H_{h,t} = S\mu(T_{in,t} - T_{out,t}) + \frac{C_a S}{\Delta t}(T_{in,t} - T_{in,t-1}) \quad (19)$$

$H_{h,t}$ -the heat load at time t, J;

heating area, m²;

μ -heat loss per unit, experience value 1.037×10^4 J/(m²°C).

3.4 Lower-Level Constraints

$$0 < e_{h,t} \leq 1 \quad (20)$$

$e_{h,t}$ is the heat satisfaction at moment t, which can be expressed as a segmental function:

$$e_{h,t} = \begin{cases} \frac{T_{in,t} - T_{in,min}}{T_{in,fit} - T_{in,min}}, & T_{in,min} \leq T_{in,t} \leq T_{in,fit} \\ \frac{T_{in,max} - T_{in,t}}{T_{in,max} - T_{in,fit}}, & T_{in,fit} < T_{in,t} \leq T_{in,max} \end{cases} \quad (21)$$

$T_{in,min}$, $T_{in,max}$ are the minimum and maximum temperatures to ensure users' thermal comfort are taken as 22 °C and 26 °C respectively, and $T_{in,fit}$ is the best comfort temperature taken as 24 °C.

4 Optimization Algorithms

In this paper, the upper layer uses a nonlinear particle swarm optimization algorithm to pass the planned collector area, heat pump rated capacity and heat storage tank capacity to the lower layer, and the lower layer collects the upper layer planning results and invokes the CPLEX toolbox to optimize the user heat load by combining basic information such as ambient temperature [13].

PSO is a classical swarm intelligence algorithm that simulates the feeding process of a flock of birds by considering the problem to be optimized as a flock of feeding birds, the solution space as the flight space of the flock, and the position of each bird in the space is a particle of the particle swarm algorithm in the solution space, which is a solution of the problem to be optimized [14]. During the evolution of the algorithm, the particles keep track of two extremes: one to the individual historical optimal position and one to the population historical optimal position. The solution process in this paper is as follows (see Fig. 5).

Step 1: input the basic data for the optimization calculation such as the light intensity data, outdoor temperature and heat load data at hourly level throughout the year, as well as the parameters of each flexibility resource and the capacity range of the flexibility resource, and set the basic parameters for the calculation such as the reasonable number of populations and the number of iterations.

Step 2: coding the variables to be solved in the planning layer with real numbers, setting the number of iterations $k = 1$ and the initial population number randomly generated as 72.

Step 3: optimizing each individual in the population, passing the corresponding configuration scheme of the system to the lower layer, and obtaining the optimal heat load profile under that configuration scheme if the constraints of the lower layer are satisfied.

Step 4: returning the heat load optimization results to the upper layer for iteration and calculating the corresponding fitness value for each individual.

Step 5: retaining the optimal individual obtained in the population, while recording the fitness value corresponding to the optimal individual.

Step 6: judge whether the maximum number of iterations 210 is reached at this point, if not, make $k = k + 1$; return to step 3, if it is satisfied, jump out of the loop and output the record of the optimal individual to get the optimal configuration scheme of the system.

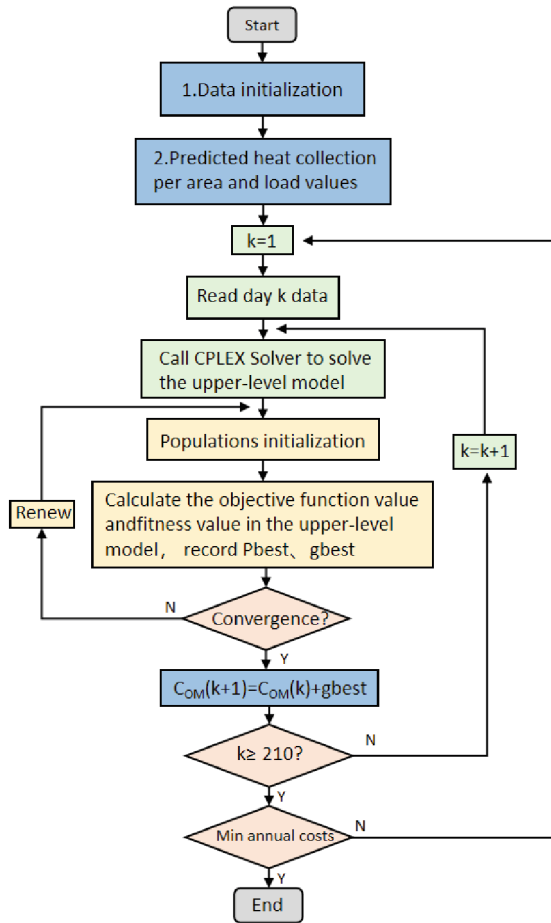


Fig. 5. Algorithm flow chart

5 Example

5.1 Load Characteristics and Peak and Valley Tariff

In order to examine the optimization of solar energy and air source heat pump parallel heating system, a pilot banner county in Ulanqab region is considered as an example, according to the county heating area of about 3 million square meters, the heating object is mainly residential home heating, and the heating period is considered as 210 days. The specific parameters of the heating installation are as follows.

In this study, the peak-valley tariff model shown in the Table 1 and Table 2 below is used for thermal storage electric heating. The daily electricity consumption time is divided into 3 periods: peak, trough and flat.

5.2 Analysis of Optimization Results

After iterative optimization, the minimum investment cost is 47,984,800 RMB and the minimum annual value of operating cost is 308,300 RMB, which is the objective function value corresponding to the best optimization variables. The corresponding optimal individuals (collector area, heat pump capacity, and water tank volume) at convergence are 1,166,400 m³, 328.37 MW, and 320 t, respectively, which is the final optimization result.

To verify the validity of the results, a comparative analysis was performed with but with optimization, and the comparative results are shown in Table 3.

Table 1. Unit configuration schedule

System parts	Main parameter	Remarks	Price
Solar collector	Thermal loss coefficient:0.47 W/m ² Collecting efficiency:0.78	Single block area of 2 m ² each 5 pieces in series	150 ¥/m ²
ASHP	Single-machine capacity $P =$ 30 kW	Jet increases enthalpy	800 ¥/kW
Storage tank		Sensible heat	1200 ¥/m ³

Table 2. Time-of-use price

State	Time	Price (¥/kWh)
Peak	8:00–12:00 18:00–23:00	0.5850
Flat	12:00–18:00 23:00–0:00	0.3672
Trough	0:00–8:00	0.1494

Table 3. Parameter comparison optimization

Optimization methods	Collector area (w/m ²)	ASHP capacity (MW)	Heat storage capacity (GJ)	Investments (¥)	Annual operating costs (¥)
Single optimization	128.8	287	216	46834.75 w	42.75 w
Synchronous optimization	132.6	353.24	256	49231.92 w	34.23 w
Bi-level optimization	116.4	328.37	248	47983.48 w	30.83 w

As can be seen from the table, the combined solar-thermal pump operating system with two layers of optimization has a significant reduction in operating costs compared to the capacity-only optimization method, although the investment costs are higher.

In the case of planning operations all using a thermal demand of 50 W/m², this paper provide a comparative analysis for demand-side response effects (see Figs. 6, 7). If user satisfaction is not considered, the internal temperature is mainly determined by the ambient temperature. After considering user satisfaction, due to the working characteristics of the storage type electric heating, the effect of comprehensive consideration, by adjusting the heating power of the storage type electric heating equipment at different times, the electric heating device generates high heat storage during the valley hours, and the heat demand is reduced during the peak hours, so that the heat load flexibly matches the time-of-use tariff, and the heat cost is reduced by 13%, and the indoor temperature is guaranteed to be within the comfort range.

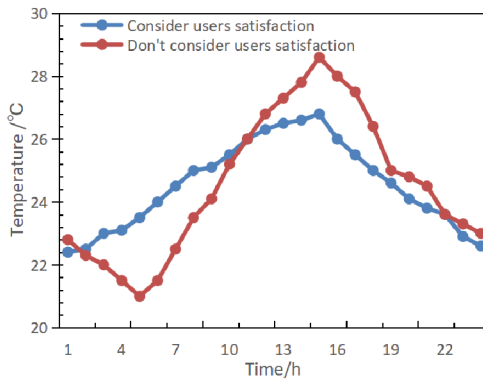


Fig. 6. Indoor temperature comparison diagram

In order to verify the effectiveness of the two-layer optimization model of the combined solar-thermal pump system considering the demand-side response, two operation scenarios of sunny day and cloudy day are further set up for analysis.

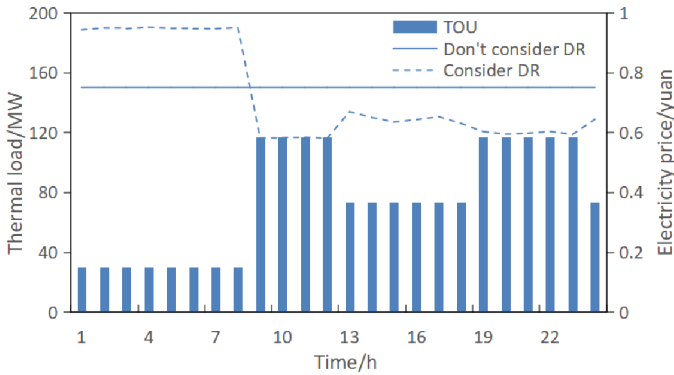


Fig. 7. Comparison of heat load optimization

The system operation output and the heat change curve of the storage tank on sunny days, which shows that the solar energy exerts heat and the storage tank stores heat during daytime, and the heat pump and storage tank jointly supply heat at night (see Fig. 8).

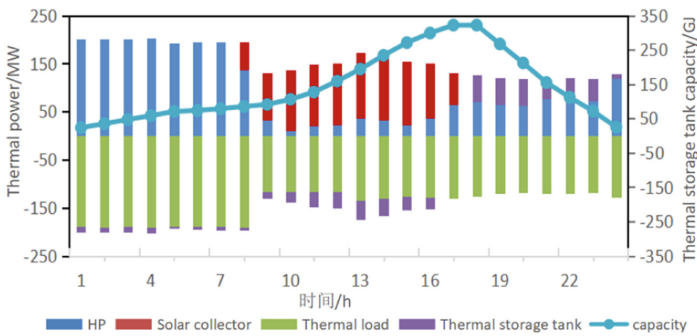


Fig. 8. Operation of the system on sunny days

The system output and the heat storage tank heat change curve on a cloudy day. From 01:00 to 08:00, the electricity price is in the valley period, the economy of electric heating equipment operation is optimal, the heat pump increases the equipment heating power, and the heat storage tank heat storage. In 09:00–12:00, the electricity price changes from valley to peak, and the solar power is insufficient on cloudy days, so the storage tank and heat pump combine to supply heat (see Fig. 9).

As shown in Table 4, the power consumption after operation optimization can save 37.5% and 0.9% on sunny days and cloudy days respectively, and the system COP can increase 16.7% and 5.1% respectively, and the heat pump COP can increase 12% and 5% respectively, which shows that the operation optimization results are reliable and the energy saving effect is obvious.

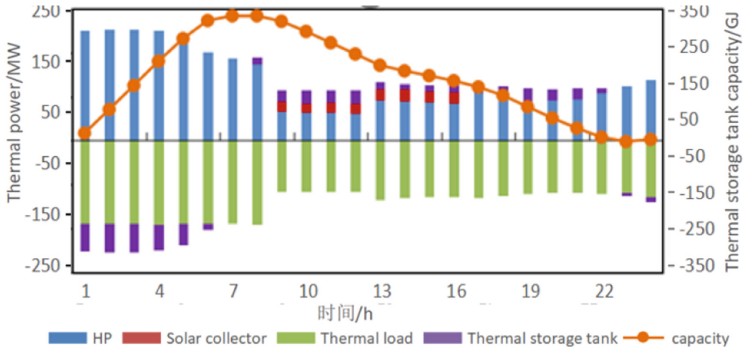


Fig. 9. Operation of the system on cloudy days

Table 4. Comparison of different scenario parameters

Method	Scene	Power consumption/kWh	System COP	ASHP COP
Single optimization	Typical day	1200	3.34	2.57
Bi-level optimization	Sunny day	911.9	3.90	2.89
	Cloudy day	1115.3	3.51	2.70

6 Conclusion

In this paper, we establish a capacity matching and operation double-layer optimization model of solar energy and air source heat pump combined operation heating system based on demand-side response, which allows users to respond under the incentive of electricity price mechanism and improves the flexibility of heating system, and capacity optimization of heat collection area, heat pump capacity and water storage tank capacity with good convergence of arithmetic process. The following conclusions are obtained through model solving and arithmetic analysis.

- (1) Combining time-of-use tariff and customer satisfaction can effectively regulate the daily residential load curve and reduce the user heating cost as much as possible while satisfying the user comfort, and at the same time, it is beneficial to reasonably plan the requirements of electricity peaking for heating devices and protect the interests of multiple parties such as grid side, environment and residential users.
- (2) The optimization results show that the economic effect of the two-layer optimization is remarkable, and the investment cost is reduced by 12,484,400 yuan compared with the simultaneous optimization method, and the operation cost can be saved by 9.9%. It shows that the optimization method in this paper can better solve the optimization problems in practical engineering.

References

1. Zou, C., He, D., Jia, C., Xiong, B., Zhao, Q., Pan, S.: Connotation, path of the world energy transformation and its significance to carbon neutrality. *J. Petroleum* **42**(02), 233–247 (2021)
2. Zhang, Z., Kang, C.: Challenges and prospects of building new power systems under the goal of carbon neutrality. *Chinese J. Electr. Eng.* **42**(08), 2806–2819 (2022)
3. Liu, Q., et al.: Optimization design of solar-assisted heating for typical rural houses in northern China. *Renew. Energy* **38**(04), 447–452 (2020)
4. Zhang, F., Wang, L., Wang, J., Jiang, C.: An experimental study on rural biogas and solar combined heating systems. *J. Solar Energy* **40**(11), 3179–3185 (2019)
5. Freeman, T.L., Mitchell, J.W., Audit, T.E.: Performance of combined solar-heat pump systems. *Sol. Energy* **22**(2), 125–135 (1979)
6. Jin, G., Chen, Z., Guo, S., Wang, J., Li, Y.: Experimental research on solar energy-air source heat pump system heating in cold areas. *Solar Energy J.* **42**(08), 251–257 (2021)
7. Zhang, X.: Simulation study of solar air source heat pump in rural Beijing]. Beijing University of Architecture and Architecture (2020)
8. Zhu, C., Liu, Y., Sun, T., Zhou, Y.: Research on Operation Optimization of Solar Energy and Air Source Heat Pump Combined Heating System. *Building thermal energy ventilation and air conditioning* **39**(04), 53–57 (2020)
9. Zong, H.: Experimental research on solar energy and low temperature air source heat pump combined heating system in cold areas. Beijing University of Architecture and Architecture (2021)
10. Xie, Y.: Analysis of the research status of flat plate type solar collector cover plate. *Energy Energy Conser.* **10**, 30–33 (2021)
11. Chen, J.: Three forms of thermal energy storage. *Energy Saving* **02**, 44 (2001)
12. Zhang, J.: Research on operation performance and optimization of solar cross-season thermal storage heating system. Shandong Jianzhu University (2020)
13. Phommixay, S., Doumbia Mamadou, L., Cui, Q.: A two-stage two-layer optimization approach for economic operation of a microgrid under a planned outage. *Sustain. Cities Society* **66** (2021)
14. Jarraya, I., Degaa, L., Rizoug, N., Chabchoub Mohamed, H., Trabelsi, H.: Comparison study between hybrid Nelder-Mead particle swarm optimization and open circuit voltage—Recursive least square for the battery parameters estimation. *J. Energy Storage* **50** (2022)